

# A Mathematical Model Based on $IC_{50}$ Curves To Predict Tumor Responses to Drugs

Catherine I. Berrouet <sup>1</sup>, Jacob Nadulek <sup>1</sup>, Emmanuel Fleurantin <sup>1</sup>, Sunil Giri <sup>1</sup>, Katarzyna A. Rejniak <sup>2</sup>, & Necibe Tuncer

Traditionally, the monolayer (two-dimensional) cell cultures are used for initial evaluation of the effectiveness of anticancer therapies. In particular, these experiments provide the  $IC_{50}$  curves that determine drug concentration that can inhibit growth of a tumor colony by half. The multicellular spheroid (three-dimensional) cultures have a histological and biochemical advantage over two-dimensional cultures for cancer models due to the fact that gene-expression patterns in spheroids are more similar to those observed in real tumor samples. However, three-dimensional cultures are time consuming, costly and laborious. Therefore, it is crucial to develop a mathematical model to investigate how to use information from the  $IC_{50}$  approach to predict how a three-dimensional tumor will respond to the treatment. One of the goals of this study is to answer the question if the  $IC_{50}$  concentration assessed from the two-dimensional cell culture will be sufficient enough to kill half off the cells in a three-dimensional spheroid? Another question is to determine whether there is a mathematical way to scale the  $IC_{50}$  concentration to be effective towards the three-dimensional case. Using the individual-cell-based model we address these questions and our results have shown that in both models as the diffusion rates increase the  $IC_{50}$  values decrease. Furthermore, the  $IC_{50}$  value for the three-dimensional model is two order of magnitude higher than the  $IC_{50}$  value of two-dimensional model. This comparison of the cellular growth in the two- and three-dimensional cases under treatment showed that if the drug diffusion rates are higher, then there is greater likelihood of reducing tumor growth using drug concentrations that are lower, hence less damaging to cancer patients.

• • •

<sup>1</sup>Florida Atlantic University, Boca Raton, Florida

<sup>2</sup>H. Lee Moffitt Cancer Center & Research Institute, Tampa, Florida

## INTRODUCTION

For many years, various clinical therapies have been developed to treat cancer. Extensive research is continually being conducted to find more efficient and less toxic treatments. Chemotherapy, the systemic administration of anticancer drugs, remains the most common form of treatment for most kinds of cancer. The three main goals for chemotherapy are to cure cancer, control the disease or possibly to palliate, and ease the symptoms caused by cancer [1]. However, chemotherapy drugs target cells at different phases of the process of forming new cells, called the cell cycle [1]. While gene expression is the process by which information from a gene is used in the synthesis of a functional gene product. These products are often proteins, which are also used in cancer research to understand the cell binding and attachments of drugs administered [2]. Understanding how these drugs work helps doctors predict which drugs are likely to work in synergism. Doctors can plan how often doses of each drug should be given based on the timing of the cell phases. Cancer cells tend to form new cells more quickly than normal cells and this makes them a better target for chemotherapy drugs [2]. However, these drugs do not differentiate between healthy cells and cancer cells. This means normal cells are damaged along with the cancer cells, and this causes side effects. For each dose of chemotherapy there needs to be a balance between killing the cancer cells (in order to cure or

control the disease) and sparing the normal cells (to lessen side effects). This is why inhibitory concentration curves are created and studied. Typically, the dose-response curve constructed, the inhibitory concentration ( $IC_x$ ) curve of a drug, can be determined by examining the effect of different concentrations of antagonist on reversing agonist activity.  $IC_{50}$  values can be calculated for a given antagonist by determining the concentration needed to inhibit half of the maximum biological response of the agonist. Furthermore,  $IC_{50}$  values can also be used to compare the potency of two antagonists [3]. In our study, the half maximal inhibitory concentration curves, denoted by  $IC_{50}$ , are the measurement of drug concentration that inhibits growth of cancer cell colony by 50% [4]. The goal of this study is to create a mathematical model to predict tumor responses to drugs based on these  $IC_{50}$  curves. We analyzed  $IC_{50}$  curves in relation to different parameters in order to maximize efficiencies in cancer drug treatments. We used the  $IC_{50}$  value generated by a two-dimensional (2D) model and to compare the tumor response in a three-dimensional (3D) model. The models are described further in section II, Methods: Developing the Mathematical Model. We hypothesized that if the drug diffusion rates are higher for both models, two-dimensional and three-dimensional case, then cellular growth will be reduced by half using higher drug concentrations.

## METHODS: DEVELOPING THE MATHEMATICAL MODEL

Our approach is to use an individual-cell-based model, that is a discrete model, coupled with diffusion equations to describe the interplay between tumor cell growth and drug uptake. First, let's discuss cell duplication. One cell cycle consists of two general phases: interphase, followed by mitosis and cytokinesis. Interphase is the period of the cell cycle

during which the cell is not dividing. The majority of cells are in interphase most of the time. Mitosis is the division of genetic material, during which the cell nucleus splits into two new fully functional nuclei. This is what we've referred to as the "mother" and two "daughter" cells. Cytokinesis divides the cytoplasm into two distinctive cells. A very elaborate

and precise system of regulation controls direct the way cells proceed from one phase to the next in the cell cycle and begin mitosis [1]. The control system involves molecules within the cell as well as external triggers. These internal and external control triggers provide “stop and advance” signals for the cell. Precise regulation of the cell cycle is critical for maintaining the health of an organism, and loss of cell cycle control can lead to cancer.

Next we discuss the development of our individual-cell-based model. To develop our discrete mathematical model, we represent cells by their nuclei and cell radius, and considered Newton's law of motion to define repulsive forces that preserve cell size, as well as the diffusive transport of drug within the cell cultures. This model is based on the work in [4]. In general, let  $C_i(t) = (x_i(t); y_i(t); z_i(t))$  and  $C_j(t) = (x_j(t); y_j(t); z_j(t))$  be the location in 3 dimensions of cells  $C_i$  and  $C_j$  at time  $t$ . By Newton's law, we have that  $F = m \cdot a$  where  $F$  is the force,  $m$  is the mass, and  $a$  represents acceleration. Acceleration is directly related to the viscosity of the medium in which the cells reside, which is a measure of a fluid's resistance or thickness. The less viscous the fluid is, the greater the fluidity or ease of movement there is within it. Hence, Newton's law used for our simulations, using MATLAB software, are coded using the equation:

$$F = m \cdot a = m \cdot \frac{d^2 C_i}{dt^2} = F_i + F_i^{\text{viscosity}} \quad (a)$$

$F_i$  is the force exerted on the  $i^{\text{th}}$  cell by their neighbors, and is a sum of forces exerted by individual cells. We define the force exerted on the  $i^{\text{th}}$  cell by the  $j^{\text{th}}$  cell to be  $f_{i,j}$ . We assume the interaction forces  $f_{i,j}$  are linear and use Hooke's Law (which states that the force needed to extend or compress a spring by some distance scales linearly with respect to that distance) with the spring constant denoted by  $F_{\text{spr}}$ . So

the equation of the forces from several neighboring cells takes the following form:

$$F_i = f_{i,j} + \dots + f_{i,N} = \sum_{j=1}^N f_{i,j} \quad (b)$$

where

$$f_{i,j} = \begin{cases} F_{\text{spr}}(2R_c - \|C_i - C_j\|) \frac{C_i - C_j}{\|C_i - C_j\|} & \text{if } \|C_i - C_j\| < 2R_c \\ 0 & \text{otherwise,} \end{cases}$$

using distance formula, between two cells  $C_i$  and  $C_j$ :

$$\|C_i - C_j\| = \sqrt{(x_i - x_j)^2 + (y_i - y_j)^2 + (z_i - z_j)^2}$$

Where radius of the cell is denoted by  $R_c$ . The number of neighboring cells are important to calculate the forces exerted on a cell during cell division and movement. Therefore, we determine the neighbor cells by checking the distance between the mother (initial) and daughter cell, using the distance formula as expressed above in (b). In other words, the neighbor cell  $C_j$  is determined by the distance between it and cell  $C_i$ . More specifically, all the cells that are within  $2R_c$  distance from  $C_i$  are all neighbors. Otherwise, if the distance by the cells  $C_i$  and  $C_j$  are greater than  $2R_c$  then the forces  $f_{i,j}$  are set to zero. Now, the viscous force is the force between a body and a fluid medium that provides resistance to cell movement. Thus, the fluid is moving in a direction opposite to the cell, that is, its drag force. From [6] we have that the viscous force is generated by a combination of cell-cell, cell-medium and cell-matrix interactions and is modeled by assuming that the drag force is proportional to its velocity (cell viscosity coefficient).

$$F_i^{\text{viscosity}} = \zeta \frac{dC_i}{dt} \quad (c)$$

Then cell relocation is governed by the following:

Since  $\frac{dC_i(t)}{dt} = \lim_{\Delta t \rightarrow 0} \frac{C_i(t+\Delta t) - C_i(t)}{\Delta t}$  in our discrete model, we approximate the derivative by its difference quotient. Hence,  $\frac{dC_i(t)}{dt} \approx \frac{C_i(t+\Delta t) - C_i(t)}{\Delta t}$ . Suppose

that  $\frac{d^2 C_i}{dt^2} = 0$ . Then by (a) and (b), we obtain:  $F_i + F_i^{viscosity} = m \cdot 0$ . Substituting (b) and (c), we have  $\sum_{j=1}^N f_{i,j}$

$$\text{Subtracting (b) from both sides} \Rightarrow \frac{\zeta C_i(t+\Delta t) - \zeta C_i(t)}{\Delta t} = -\sum_{j=1}^N f_{i,j}$$

$$\text{Multiplying both sides by } \Delta t \Rightarrow \zeta C_i(t + \Delta t) - \zeta C_i(t) = -\Delta t \sum_{j=1}^N f_{i,j}$$

$$\text{Adding } \zeta C_i(t) \text{ to both sides} \Rightarrow \zeta C_i(t + \Delta t) = \zeta C_i(t) - \Delta t \sum_{j=1}^N f_{i,j}$$

$$\text{Finally, we have our equation for cell relocation } C_i(t + \Delta t) = C_i(t) - \frac{\Delta t}{\zeta} \sum_{j=1}^N f_{i,j}$$

Recall, we let  $C_i(t) = (x_i(t), y_i(t), z_i(t))$  and  $C_j(t) = (x_j(t), y_j(t), z_j(t))$  be the location in 3 dimensions of cells  $C_i$  and  $C_j$  at time  $t$ . Now, from [5], each cell  $C_i(t)$  is defined by its position  $(x_i(t), y_i(t), z_i(t))$ , and is characterized by several properties, such as current cell age  $C_i^{age}$ , and cell maturation age at which the cell is ready to divide, we denote as  $C_i^{mat}$ . When the cell  $C_i(t)$  divides, one of its daughter cells  $C_{i_1}(t)$  takes the coordinates of its mother cell, we represent this behavior like so in our MATLAB code:

$$(x_{i_1}(t), y_{i_1}(t), z_{i_1}(t)) = (x_i(t), y_i(t), z_i(t))$$

whereas the second daughter cell is placed randomly near the mother cell:

$$(x_{i_2}(t), y_{i_2}(t), z_{i_2}(t)) = (x_i(t), y_i(t), z_i(t)) + \begin{pmatrix} \Delta x \\ \Delta y \\ \Delta z \end{pmatrix}_{\substack{\square \\ \text{determined randomly}}}$$

Initially, the current age of both daughter cells is set to 0, and the cell maturation age is inherited with a

small noise term. This means cells that reach maturation age divides and splits into its daughter cells, the daughter cells replace the position of the mother cell with the same random noise. Drug kinetics within the computational domain and its cellular uptake are defined as follows: Let  $u((x(t), y(t), z(t)))$  represent the drug concentration at position  $(x(t), y(t), z(t))$  at time  $t$ . Let  $D_u$  denote the drug diffusion coefficient,  $\rho_u$  drug uptake rate, and  $d_u$  drug decay rate, and let  $C_i^u(t)$  denote the amount of drug concentration of the  $i^{th}$  cell at time  $t$ . Then the rate of change of the drug concentration on the  $i^{th}$  cell is given by  $\frac{dC_i^u}{dt}$  which is

$$\frac{dC_i^u}{dt} = \text{input rate of drug} - \text{output of drug.}$$

$$\frac{dC_i^u}{dt} = \max \left( 0, \sum_{n \text{ drug}} \min([u(x(t), y(t), z(t))], \rho_u) - d_u C_i^u(t) \right)$$

uptake                      decay

Similarly,  $\frac{dC_i^u}{dt}$  is approximated by its difference quotient,

$$\frac{C_i^u(t+\Delta t) - C_i^u(t)}{\Delta t} = \max \left( 0, \sum_{(x,y,z)} \min[u(x(t), y(t), z(t)), \rho_u] - d_u C_i^u(t) \right)$$

$$C_i^u(t + \Delta t) - C_i^u(t) = \Delta t [\max(0, \sum_{(x,y,z)} \min[u(x(t), y(t), z(t)), \rho_u] - d_u C_i^u(t))]$$

$$C_i^u(t + \Delta t) = C_i^u(t) + \Delta t [\max(0, \sum_{(x,y,z)} \min[u(x(t), y(t), z(t)), \rho_u] - d_u C_i^u(t))] \quad (2)$$

We now look at drug diffusion. We assume that the diffusion coefficient,  $D_u$ , is constant, and does not dependent on time. Let  $u(x(t), y(t), z(t))$  be the drug concentration at position  $(x(t), y(t), z(t))$  at time  $t$ . From Fick's Law we approximate the

second partial derivative  $\frac{\partial^2 u}{\partial x^2}$  by second order centered finite difference formula which is given by  $\frac{\partial^2 u}{\partial x^2} \approx \frac{u(x+\Delta x, y, z) - 2u(x, y, z) + u(x-\Delta x, y, z)}{(\Delta x)^2}$ . Hence, we obtain  $\frac{\partial u}{\partial t} = D_u \left( \frac{\partial^2 u}{\partial x^2} + \frac{\partial^2 u}{\partial y^2} + \frac{\partial^2 u}{\partial z^2} \right)$  That is:

$$\begin{aligned} \frac{u(x(t+\Delta t), y(t+\Delta t), z(t+\Delta t)) - u(x(t), y(t), z(t))}{\Delta t} = \\ D_u \left( \frac{u(x+\Delta x, y, z) - 2u(x, y, z) + u(x-\Delta x, y, z)}{(\Delta x)^2} + \frac{u(x, y+\Delta y, z) - 2u(x, y, z) + u(x, y-\Delta y, z)}{(\Delta y)^2} \right. \\ \left. + \frac{u(x, y, z+\Delta z) - 2u(x, y, z) + u(x, y, z-\Delta z)}{(\Delta z)^2} \right) \end{aligned} \quad (3)$$

Let  $u(x(0), y(0), z(0)) = u_0(x, y, z)$  denote the initial drug concentration. Using the individual-cell-based model equations (a) -- (3), we implemented two models in MATLAB, which we refer them as 2D and 3D models. In the 2D model, the drug concentration is evenly distributed to the whole domain where the cells are located (since cells are defined as its location). In the 3D model the drug is administered from the boundary of the domain and drug diffuses to the cells. The 2D model represents the Petri dish experiments (see Figure 1(a)) and the 3D model represents the cross-section through the three-dimensional spheroids (see Figure 1(b)). Using these two models we conducted several simulations to analyze in depth cellular responses to the drug dosage administered. Equations 1-3 are implemented in MATLAB to run the simulations. Each simulation represents a 72 hour period of cellular growth after a specific drug dosage is administered. Cells duplicate so the number of cells in the domain changes in time. So to compute  $IC_{50}$  curves, we count the number of cells remaining after 72 hours (hence, we record the number of cells remaining after each simulation).

Now we discuss the parameters used for our model. The standard procedure for growing

cell colonies in monolayers (in a Petri dish) uses a 72-hour time frame [1]. To create a realistic initial cell count for our discrete model, we began to analyze cellular growth and how cells duplicate with respect to time. For our model, cellular growth is dependent upon drug absorption and cellular movement. Using MATLAB to run our two-dimensional and three-dimensional models, we recorded the number of cells remaining after the simulated 72 hours when no drug was administered, the 2D model generated 285 cells while the 3D model generated 165 cells, setting these value as our normalization cell count for all future simulations (Chart 1) respectively. Our first initial set of simulations were to focus on the effects of drug dosage alone. Thus, we fixed the diffusion coefficient,  $D_u = 0.75$ , for each simulation that tested various drug dosage ( $u_0(x, y, z)$ ) (Figure 2). After completing a set of simulations, we then generated our  $IC_{50}$  curve. Each  $IC_{50}$  curve is computed in the following way: each point plotted is a computed ratio between the initial cell count (normalization cell count) and the cells that remained at the end of the 72-hour simulation. Hence, each point plotted is the representative percentage of cells after one complete simulation, according to its respective administered drug dosage. Next, we recorded a set

of simulations with fixed diffusion coefficients and varying drug dosages (Figure 4 & 5). For numerous diffusion coefficients fixed between 0 and 1 (Figure 5 & 6), we tested each  $D_u$  with different drug dosages ( $u_0(x, y, z)$ ). Then the inhibitory concentration curves were generated for each of these cases as well. As a pseudo-algorithm: in all 2D cases we seed 285 number of cells; while in all 3D cases we seed 156 number of cells. And the initial drug concentration ( $u_0(x, y, z)$ ) was varied between 0.01 and 0.09

## RESULTS

Without any drug administered to the system, that is, setting ( $u_0(x, y, z)$ ), there were at least 84 cells generated on average from 24 to 36 hours (Chart 1). From the simulations throughout each time interval: for time (t) in hours, when  $t=24$  there are about 90 cells generated, when  $t=24 \times C^{98\%}$  there were 83 cells generated, and when  $t=36$ , there were about 79 cells generated. Where  $C^{98\%}$  is randomly generated (determined by using the MATLAB rand function which uses a uniform distribution). Hence, for both models, we fixed the initial cell count at 100. Now, to test drug effectiveness, is to count how many cells die when exposed to various drug concentrations. Dose refers to the amount of a substance that is introduced to the organism. Generally, different drug doses can exert very different effects on the growing cells. Very low doses of some compounds can even induce stronger cellular responses than much higher doses and may result in different killing impacts. In Figures 2 and 3 we examine cellular responses to gradually increasing drug dosages in both the 2D and 3D models, and determine the  $IC_{50}$  value in both cases. These simulations indicate that in the 2D model drug dosage necessary to kill half of the initial population is much smaller in comparison to the drug dosage amounts necessary in the 3D model. In fact it is two order of magnitude smaller. These results led us to our next question: How does

for 2D model in different simulations (respective to each drug dosage administered). Similarly, in 3D, the initial drug concentration was varied between 0.1 and 100, in different simulations. All model parameters are summarized in Table 1. This mathematical model has been discretized using the standard finite difference methods, and parameters were chosen such that the numerical stability is preserved ( $D_u \Delta t / (\Delta x)^2 \leq \frac{1}{2}$ ), where  $\Delta t$  and  $\Delta x$  are the numerical time step and grid width, respectively.

this relate to diffusion? Since diffusion is the process by which molecules of higher concentration move to areas of lower concentration, we varied  $D_u$  (the diffusion coefficients) over a range of values and analyzed how the inhibitory curves changed with increasing drug dosages. Figures 4 and 5 show the  $IC_{50}$  curves generated for various diffusion coefficients over the same ranges of drug dosage. All cell counts are normalized to the number of cells surviving a very small drug dosage of 0.01mg. In the three-dimensional model, with a very small drug dosage of 5mg,  $D_u=0.85$  and  $D_u=1$  significantly reduced cell population by more than 40%. However, for all, as drug dosage increased, the percentage of reduced cellular growth became constant (See Figure 5). In summary, diffusion coefficients larger than 0.35, reduced the percentage of cellular growth, resulting in lower inhibitory concentration curve percentage values. While all  $D_u$  in the two-dimensional model, none of the  $IC_{50}$  curves reach 50%. That is, the diffusion coefficients ( $D_u$ ) smaller than 0.1 in the two-dimensional model did not ever reduce cellular growth by 50%. While the diffusion coefficients smaller than 0.75 in the three-dimensional model did not reduce cellular growth by 50%, we see that the  $IC_{50}$  curves became constant.

CHARTS AND FIGURES

Table 1:Parameters

Parameters	Terms	Initial Values
$D_u$	diffusion coefficient	0.01-0.90
$\rho_u$	drug uptake	0.01-50
	cell diameter	5 microns (5.00+e00)
$R_C$	cell radius	10 microns
$F_{spr}$	spring constant	1.00+E00
$t$	time	72 hours
$F_i^{viscosity}$	mass/viscosity	1.00e+01 nu
$\sum_{j=1}^N f_{i,j}$	max neighboring cells	N=10
2D model	boundary drug conditions	0.02
3D model	boundary drug conditions	0.5
$d_u C_i^u(t)$	decay (cell toxicity threshold)	0.75
mg	micrograms per milliliter	drug dosage

# CHART 1: CELL GROWTH IN 2D

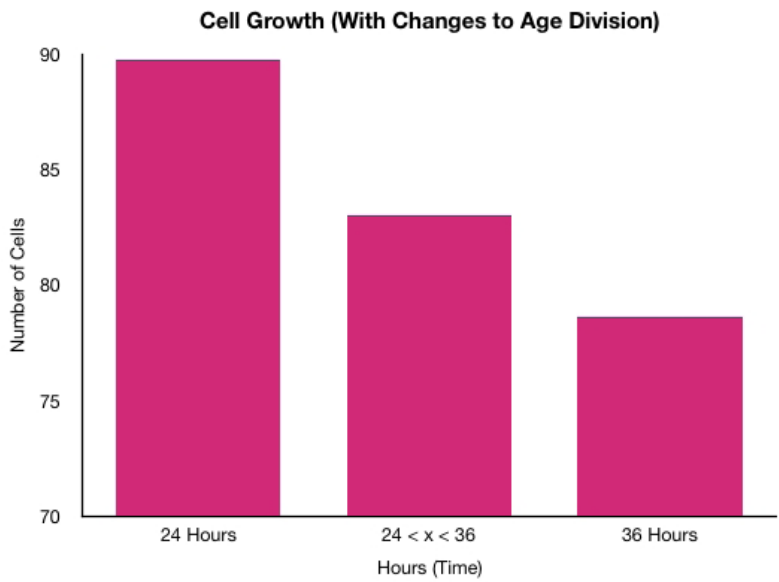
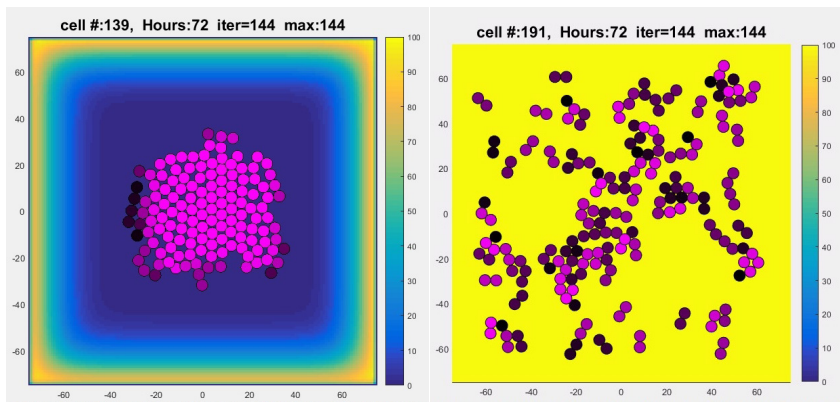


**Chart 1.** Two-dimensional model was used to test different time parameters, minimum time  $t=24$ , maximum time  $t=36$ , and analyze the cellular growth with each respective time frame in order to set a control cell count for all future simulations.

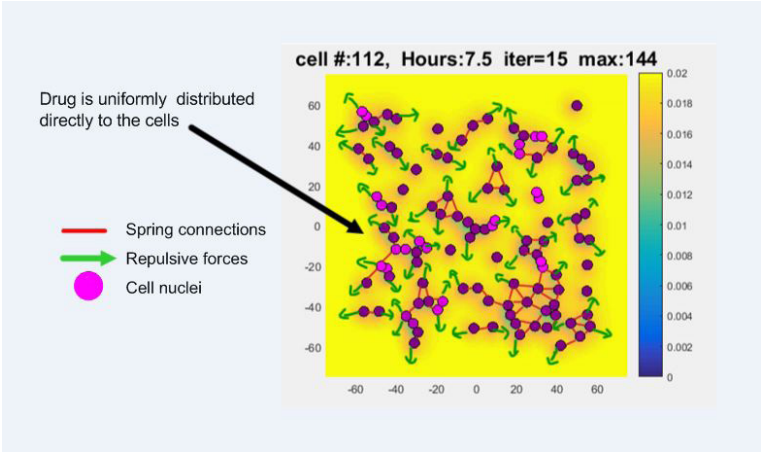
## Two Computational Models



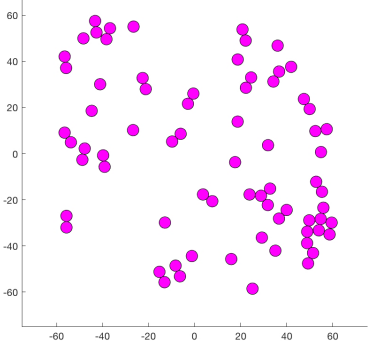
Three dimensional model simulations show the diffusion gradient of teh drug through the blue hues, while teh cells that accumulate the drug die off (by the purple hues that turn darker and darker).

Two Dimensional Model Simulations show the direct distribution of the drug directly administered to all the cells (yellow gradient) and the cells die off (by purple hues that turn darker and darker).

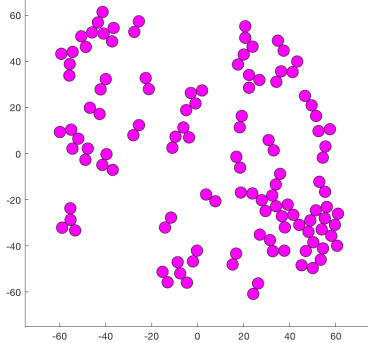




conc:0 cell #:72, Hours:6.944 iter=5000 max:51840



conc:0 cell #:120, Hours:13.89 iter=10000 max:51840



conc:0 cell #:166, Hours:20.83 iter=15000 max:51840

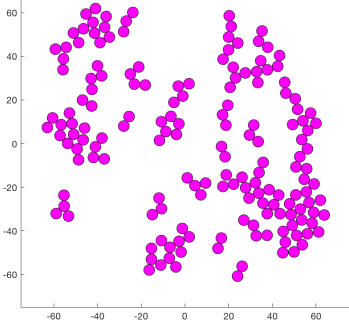


**Figure 1(a). Two-Dimensional Model.** Computational representation of a Petri dish in which individual cells are seeded and allowed to grow and migrate (referred to as the 2D model). In the 2D model the drug is administered to the cells directly without having to permeate the boarder of the cells. In which diffusion occurs strongly since the cells are in a two-dimensional space (the petri dishes), thus the cells are much more spread out [8]. The progression of cells generated (cell duplication) from the initial fifty cells seeded are demonstrated in the three mini freeze frames of our simulations.

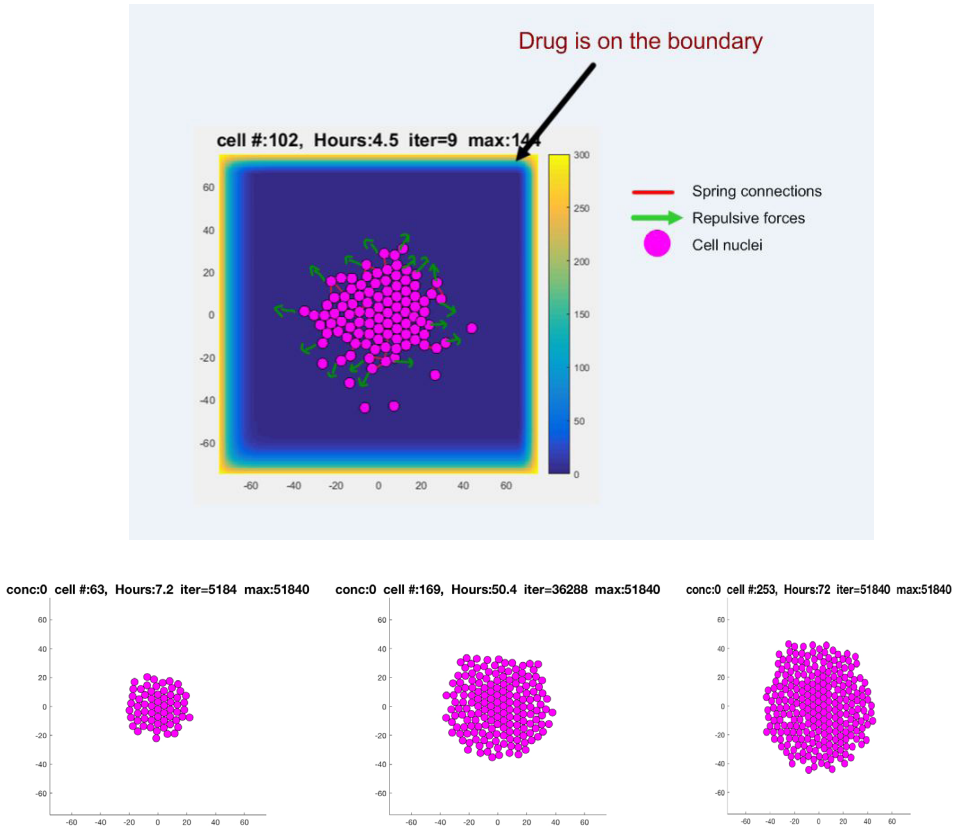


**Figure 1(b). Three-Dimensional Model .** Computational representation of the central cross-section through the cell spheroid (referred as 3D model). In the 3D model the drugs permeate the cells boarding the entire cluster. The cells represent a colony in which the cells cluster together. It shows the aggregation of the cells, which is the property of spheroids in which the code is designed to mimic. The progression of cell generation (aggregation from cell duplication) in the spheroid is demonstrated in the three mini freeze frames from of our simulations.

In both images, Figure 1(a) and Figure 1(b), the pink circles represent the cells, the red segments represent spring connections between neighboring cells. Note, that there are no connections if the cells are far apart. Green arrows represent the cumulative forces exerted on the cells and the direction of cell movement. The gradient of colors are supposed to illustrate the cells that reach a concentration threshold causing the cell to die from the drugs administered.

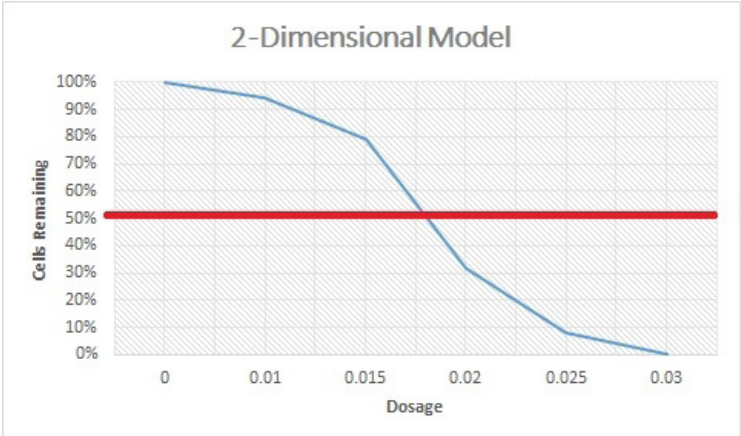


**Figure 2. 2D Drug Dosage & Fixed  $D_u=0.75$ .**  $IC_{50}$  curve generated for 2D model (Petri dish setting) for a fixed diffusion. Coefficient of  $D_u=0.75$ , and drug dosages between 0 and 0.03.

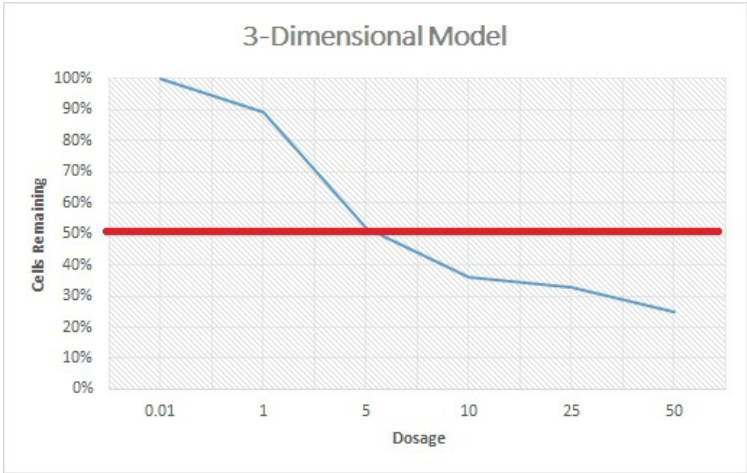


**Figure 3. 3D Drug Dosage & Fixed  $D_u=0.75$ .**  $IC_{50}$  curve generated for 3D model (cross-section through the 3D spheroid) for a fixed  $D_u=0.75$  and drug dosages between 0.01 and 50.

Comparing the 2D model (Figure 2) with the 3D model (Figure 3) Drug Dosages: the graphs represent the inhibitory curves at a fixed diffusion coefficient of 0.75 for testing various drug concentration levels. The two dimensional and three dimensional curves are generated to compare and contrast the dosage levels necessary to inhibit cellular growth in relation to both models.

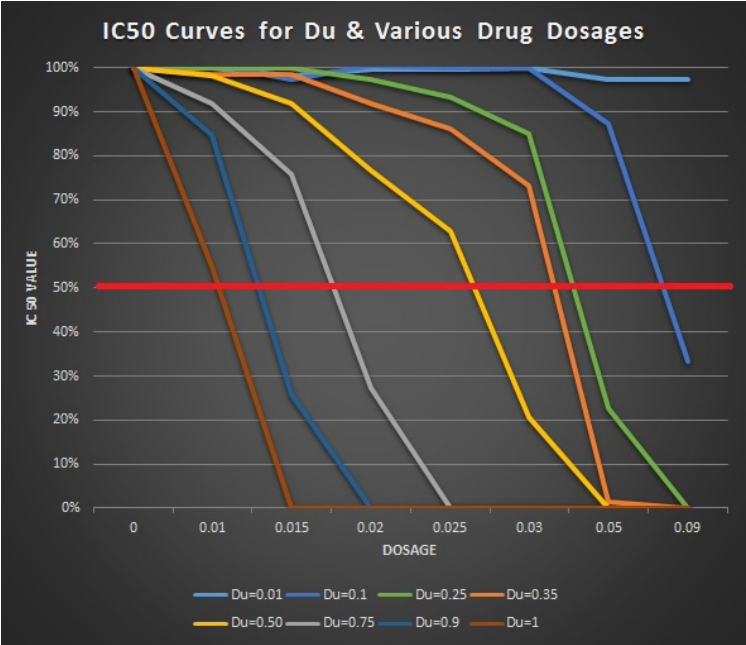


Figure 4. 2D Drug Dosage & Fixed  $D_u$ .

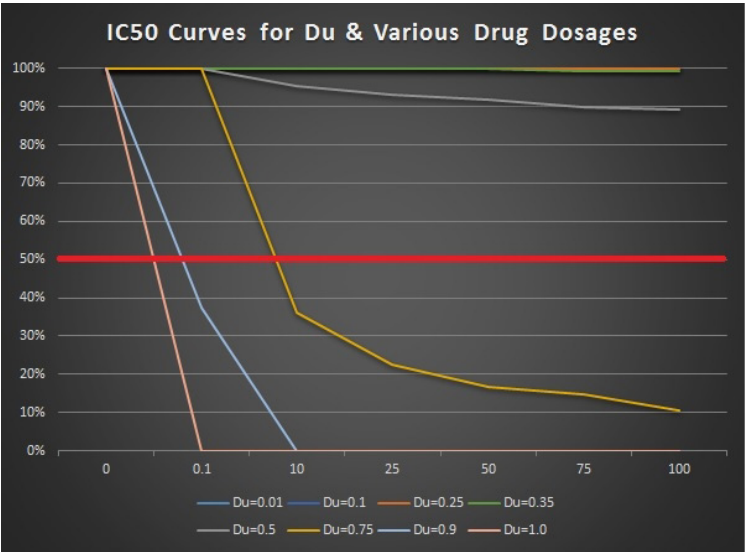


Figure 5. 3D Drug Dosage & Fixed  $D_u$ .

Comparing the 2D model (Figure 4) with the 3D model (Figure 5) Diffusion Coefficients at various drug dosages: instead of having one fixed  $D_u$  for each model, different diffusion coefficients were tested to compare the drug dosages tested at generated graphs respectively.

## DISCUSSION

Our results do not support our hypothesis that higher diffusion rates in both cases will yield less cellular growth with respect to higher drug concentrations. In fact, we saw that the larger diffusion coefficients paired with lower drug dosages inhibited at least half the cellular population much faster than the smaller diffusion coefficients paired with lower drug dosages. In other words, smaller  $IC_{50}$  values generated from both two-dimensional and three-dimensional inhibitory drug-dosage curves resulted from low drug concentrations that had higher diffusion rates. This gives the notion that cellular death does somewhat depend on how much and how fast diffusion occurs [2]. The smaller diffusion coefficients had very large  $IC_{50}$  curve percentages with respect to very low dosages in both models. In the two-dimensional model, as the diffusion coefficients increased, the inhibitory curve began to form a declining slope. It kept 90% of the cells at a very large dosage and continued to inhibit cellular growth by retaining more than 50% at a dosage of 10mg and lower. Similarly, in the three-dimensional model, when  $D_u=0.75$ , a much larger diffusion coefficient retained less than 50% of the cells when dosage was 10mg or less. Although our data does not support our prediction that larger diffusion coefficients yield more cellular growth with respect to higher drug dosages; the results do suggest that diffusion does play a part in drug effectiveness and whether cellular inhibition is achieved or not. Furthermore, since the process of diffusion is whereby materials are exchanged between a cell and its environment, then the rate of diffusion is affected by temperature, size of molecules, and the steepness of the concentration gradient [2]. Since the two-dimensional model represents cell colony growth in a two-dimensional petri dish, there is a higher concentration gradient as the cells duplicate, the diffusion amongst

the cells would be affected less by the force within the cells, but more by their small environment, thus killed off more cells with very small drug dosages. However, the three-dimensional model represents a cross-section through a spheroid, which are aggregates of tumor cells without blood vessels, which retain many properties of solid tumors [1]. Hence, we must consider the fact that the three-dimensional model contains cells which are more compact and have more dense spatial structure compared to the two-dimensional model. The diffusion coefficient may have less impact with drug dosages, thus does not inhibit cellular growth as much over increased drug dosage. This may suggest the possibility of resistance over time towards a drug.

In conclusion, the parameters may seem to have intuitively obvious relationships, while in other situations there may be very weak signals in very meaningless data. However, there is a huge range of applications for our data. Our data explicitly showed that the average dosage necessary to inhibit at least 50% of cellular growth, for the three-dimensional model was two thousand times larger than the average dosage necessary in two-dimensional model. Our findings are consistent with previous comparative results in literature such like [1] that compare three-dimensional spheroid drug responses to two-dimensional cellular (petri dish setting) cellular drug response. It must be noted that a result like this could save many lives over the long run and be worth millions of dollars in profits if it results in the drug's approval for widespread use. Hence, this brings considerable questions for future studies and goals for further experimentation: If there is a mathematical way to scale the two-dimensionally generated  $IC_{50}$  concentration to the three-dimensional case? Considering different cell types, since there are various forms of cancer, how do these diffusion coefficients change

depending on the drug? What are the probabilities that long-term, low-level exposures to these drugs will cause other disease? To what extent does the drug diffusion in cells affect the initial genetic cellular interstitial materials? What are the probabilities of other impacts in those exposed to low doses of the drugs used? Is there any evidence of potential links between exposures at early developmental stages and health impacts later in life? How does the diffusion coefficient affect the nutritional balance within

nanoparticles and cellular metabolism? Finding the way to utilize the two-dimensionally-generated  $IC_{50}$  value in the three-dimensional spheroid or mice experiments will help biologists to design more efficient laboratory experiments. If additional time were permitted our future goals for this study would be to build a two-dimensional model with the intent to simulate a spheroid slice infused into a diffusive medium and analyze the drug diffusion in comparison to the three-dimensional case.

## ACKNOWLEDGEMENTS

Acknowledgements goes to the PIC Math program. PIC Math is a program of the Mathematical Association of America (MAA) and the Society for Industrial and Applied Mathematics (SIAM). Support is provided by the National Science Foundation (NSF grant DMS-1345499).

We also express our deepest gratitude to Dr. Necibe Tuncer and would like to acknowledge her for all the supervision, support, and guidance throughout our research.

## REFERENCES

- [1] The American Cancer Society Medical and editorial Content Team. Last Revised: Feb 16, 2016, from [https://www.cancer.org/treatment/treatments-and-side-effects/treatment-types/chemotherapy/how-is-chemotherapy-used-to-treat-cancer.html#written\\_by](https://www.cancer.org/treatment/treatments-and-side-effects/treatment-types/chemotherapy/how-is-chemotherapy-used-to-treat-cancer.html#written_by). Accessed March 23, 2017.
- [2] Y. Gao, M. Li, B. Chen, Z. Shen, P. Guo, M. G. Wientjes, and J. L.-S. Au. Predictive models of diffusive nanoparticle transport in 3-dimensional tumor cell spheroids. *The AAPS journal*, 15(3):816-831, 2013.
- [3] Wikipedia contributors.  $IC_{50}$ . Wikipedia, The Free Encyclopedia. August 31, 2017, 23:30 UTC. Available at: <https://en.wikipedia.org/w/index.php?title=IC50&oldid=798274340>. Accessed September 19, 2017.
- [4] S. N. Gardner. A mechanistic, predictive model of dose-response curves for cell cycle phase-specific and-nonspecific drugs. *Cancer research*, 60(5):1417-1425, 2000.
- [5] J. Perez-Velazquez, J. L. Gevertz, A. Karolak, and K. A. Rejniak. Microenvironmental niches and sanctuaries: A route to acquired resistance. In *Systems Biology of Tumor Microenvironment*, pages 149-164. Springer, 2016.
- [6] Philip J. Murray, Carina M. Edwards, Marcus J. Tindall, and Philip K. Maini. From a discrete to a continuum model of cell dynamics in one dimension. In *Physical Review*, E 80, 031912, 2009.
- [7] Trautmann, N. (n.d.). The Dose Makes the Poison—Or Does It? Retrieved March 23, 2017, from <http://www.actionbioscience.org/environment/trautmann.html>

- [8] Narges K. Tafreshi, Ariosto Silva, Veronica C. Estrella, Timothy W. McCardle, Tingan Chen, Yolaine Jeune-Smith, Mark C. Lloyd, Steven A. Enkemann, Keiran S. M. Smalley, Vernon K. Sondak, Josef Vagner, and David L. Morse. In Vivo and in Silico Pharmacokinetics and Biodistribution of a Melanocortin Receptor 1 Targeted Agent in Preclinical Models of Melanoma. *Mol. Pharmaceutics* 2013, 10, 31753185
- [9] Rejniak, K. A. and Anderson, A. R. A. (2011), Hybrid models of tumor growth. *WIREs Syst Biol Med*, 3: 115–125. doi:10.1002/wsbm.102
- [10] J. Friedrich, C. Seidel, R. Ebner and L.A. Kunz-Schughart. Spheroid-based drug screen: considerations and practical approach. *Nature protocols*, 4(3):309-324, 2009.